

PLANETARY NEBULAE AS STANDARD CANDLES. VI.
A TEST IN THE MAGELLANIC CLOUDS

GEORGE H. JACOBY

Kitt Peak National Observatory, National Optical Astronomy Observatories¹

ALISTAIR R. WALKER

Cerro Tololo Inter-American Observatory, National Optical Astronomy Observatories¹

AND

ROBIN CIARDULLO

Kitt Peak National Observatory, National Optical Astronomy Observatories¹

Received 1990 April 7; accepted 1990 June 18

ABSTRACT

We have measured the [O III] $\lambda 5007$ fluxes of the brightest planetaries in the LMC (102 objects) and SMC (31 objects) using narrow-band imaging at the CTIO 0.9 m telescope. Our fluxes agree to $\sim 5\%$ with photoelectric measurements available in the literature (31 objects); agreement is much worse for objects with only spectrophotometric observations.

Using the fluxes for the complete sample of bright LMC planetaries, we derive a distance using the planetary nebula luminosity function (PNLF). If we adopt a foreground plus internal reddening of $E(B-V) = 0.10$ for the LMC, which is based on direct measurements of the Balmer decrement of several planetaries, and estimates from B stars, clusters, and H I measurements, we find the distance modulus to be 18.44 ± 0.18 . This agrees superbly with the Cepheid distance modulus of 18.47 ± 0.15 (Feast and Walker) and estimates between 18.2 and 18.5 from RR Lyrae stars, Miras, OB stars, and clusters. Similarly for the SMC, we adopt $E(B-V) = 0.06$ and derive a distance modulus of $19.09^{+0.25}_{-0.32}$.

The excellent consistency between the PNLF distance to the LMC, which uses the bulge of M31 as its sole calibrator, and the Cepheid distance is very strong evidence that the method is insensitive to host galaxy Hubble type, color, or metallicity.

Subject headings: galaxies: distances — galaxies: Magellanic Clouds — luminosity function — nebulae: planetary

I. INTRODUCTION

The bright end of the planetary nebula (PN) luminosity function (PNLF) has been shown to be an accurate standard candle for early-type galaxies (Jacoby 1989; Ciardullo *et al.* 1989; Jacoby *et al.* 1989; Ciardullo, Jacoby, and Ford 1989; and Jacoby, Ciardullo, and Ford 1990). In M81, the PNLF method yields distances in very good agreement with other reliable techniques (e.g., Cepheids), and PNLF distances to galaxies in the Leo and Virgo clusters show excellent internal consistency. However, two potentially important issues have not yet been adequately addressed. First, the PNLF method is a secondary distance indicator, and only M31 has been used to set the zero point. From the dispersion in the various distance estimates given in Table 4 of Mould (1988), the adopted M31 distance modulus of 24.26, based on infrared photometry of Cepheids (Welch *et al.* 1986), appears secure to about 0.15 mag. However, because this uncertainty propagates into all PNLF distances, another calibrator galaxy is highly desirable.

The second issue concerns the dependence of the PNLF on Hubble type. Although the PNLF method is most easily applied to E and S0 galaxies, the calibrator (M31) is an Sb galaxy. Unfortunately, there is no early-type galaxy with a well-determined distance suitable for testing the applicability of this calibrator. We can, however, investigate the sensitivity

of PNLF distances to changes in Hubble type in later, rather than earlier, type galaxies. The ideal place to examine this question is in the Magellanic Clouds (hereafter, MC), and in particular, the LMC.

A PNLF distance to the LMC serves two purposes. If the derived distance were to agree with that found by more traditional standard candles (e.g., Cepheids, RR Lyraes, Miras, cluster color-magnitude diagrams), it would provide strong support for the use of the PNLF in galaxies of all Hubble types. More importantly, since the LMC PN have chemical compositions (Monk, Barlow, and Clegg 1988) much lower than those found in M31 (Jacoby and Ford 1986), a consistent PNLF distance would strengthen the argument that this distance indicator is metallicity insensitive. A comparison of the PNLF distance to the LMC with that of other distance indicators is therefore of considerable interest.

In this paper, we use the LMC and SMC as proving grounds to explore these issues. In § II, we describe our sample selection and photometric results. In § III, we compare our derived distances with those determined from more classical methods and discuss how these results impact the use of PN for extragalactic distances.

II. OBSERVATIONS

a) *The Sample of Planetary Nebulae*

There have been several surveys of the MC, some specifically aimed at finding PN and others being general searches for emission-line objects. Early work on identifying MC PN, prin-

¹ The National Optical Astronomy Observatories are operated by the Association of Universities for Research in Astronomy, Inc., under cooperative agreement with the National Science Foundation.

cipally by Henize (1956) and Lindsay (1961, 1963) has been comprehensively summarized by Westerlund (1968). No more searches for MC PN were made for more than a decade until the thorough survey carried out by Sanduleak, MacConnell, and Philip (1978) (henceforth SMP). They obtained objective prism plates with the Michigan Schmidt telescope at CTIO, and measured the [O III] and hydrogen emission lines of objects over the entire fields of the SMC and LMC, with the exception of only the most outlying regions. A total of 102 LMC and 28 SMC PN were identified, 25 of which were new discoveries. Supplementary work (Sanduleak and Pesch 1981) identified several more candidates in the SMC, but only two of these subsequently turned out to be PN (Dopita *et al.* 1985; Morgan and Good 1985). Later surveys with larger telescopes, using both on-band/off-band filter and objective prism techniques by Jacoby (1980) and Morgan and Good (1985) have failed to find any additional luminous PN, so it is likely that the first 2 magnitudes of the [O III] luminosity function are statistically complete. (The low-excitation SMC PN, Lindsay 302 [Lindsay 1961], lies outside the SMP search area.)

We chose those objects listed by SMP for our sample of PN, together with the two SMC PN from Sanduleak and Pesch (1981) and Lindsay 302. Approximate positions for these objects and finding charts for the SMC PN are given by SMP and Sanduleak and Pesch (1981). Accurate positions for most of the LMC PN are given by Meatheringham *et al.* (1988). SMP did not include finding charts for the LMC PN; however, charts for 64 of these can be found in the original survey papers (cf. Henize 1956), albeit at small scale. The PN lacking finding charts were discovered (again!) in the course of this project; finding charts for all objects are given in Figures 1 and 2 (Plates 22–30).

b) Observations

The PN were reidentified using the on-band/off-band technique described in earlier papers in this series. To summarize, an [O III] image was obtained at each PN position using a narrow-band (FWHM 28 Å) filter with a central wavelength near 5012 Å at the observing temperature (typically 9°C). These images were compared with images taken through a continuum filter centered near 5300 Å (FWHM 275 Å). The PN were invariably the brightest objects in the on-band images and almost invisible on the off-band frames.

Observations were made at the $f/13.5$ focus of the CTIO 0.9 m telescope during six nights in 1989 November and December. All the nights were photometric with seeing FWHM between 1".2 and 1".7. A Tektronix 512 × 512 (Tek No. 3) CCD, which has a pixel size of 0".45 and a field of view of 230" square, was used for all the observations. (Tek No. 3 is a thinned, back-side illuminated CCD without the implant and antireflection coating that characterizes the most recent Tektronix devices.) Exposure times were typically 100 s (off-band) and 400 s (on-band), although for some of the fainter SMC PN, on-band exposures as long as 1000 s were required.

Typically five measurements were made each night of the spectrophotometric standard stars LTT 377 and EG 21 (Stone and Baldwin 1983) in order to establish zero points and measure the atmospheric extinction.

c) Reductions

For distant galaxies it is usually helpful to subtract a scaled off-band image from the on-band image in order to reduce the effect of crowding and to remove gradients from the diffuse

light of the host galaxy. At the distance of the MC, these effects are unimportant; hence the off-band frames were used only to ensure correct identification of the PN.

The brightness of the PN on the [O III] frames made measurement very easy, and a simple aperture photometry procedure was adopted. The PN were measured through an aperture with radius 6".3, and the sky background was measured through a surrounding annulus having inner and outer radii of 8".1 and 11".3. Standard stars were measured in precisely the same way; the standard star photometry is summarized in Table 1. Column (1) is the UT date of the observation, column (2) is the number of standard star observations over the night, and column (3) is the derived atmospheric extinction (in mag-airmass⁻¹). Column (4) is the average value for the zero-point correction, which is defined as the difference between the instrumental magnitude of the standard stars (corrected for atmospheric extinction) and their monochromatic magnitudes at 5012 Å derived by interpolating in the tables of Stone and Baldwin (1983). The 1 σ standard deviation of the zero-point measurements is given in column (5). (Poisson statistics of the star and sky counts imply that these errors should be 0.002–0.003 mag.)

The zero-point correction is nearly constant for the last five nights but indicates that the system was ~ 0.07 mag less sensitive on the night of November 10. For that particular night an attempt was made to increase the sensitivity of the CCD with a UV flood treatment (Ditsler 1990; Oke *et al.* 1988). Unfortunately, this procedure did not have the desired effect, and, in fact, appears to have decreased the CCD quantum efficiency. The CCD was recycled to room temperature and pressure following November 10 and the CCD quantum efficiency returned to its normal value.) As has been pointed out elsewhere (e.g., Walker 1984), the impressive stability of CCD systems can be an aid in evaluating the extinction, since for an observing run of several contiguous nights the instrumental zero point can be assumed to be constant.

In order to convert emission-line sources to the flux system defined by stellar (i.e., continuum) sources, it is necessary to have an accurate representation of the filter response curve (Jacoby, Quigley, and Africano 1987). We therefore measured the on-band filter transmission after the observing runs to guard against changes with age. (Although the characteristics of this filter have remained constant since 1988, the filter did shift to the blue by nearly 3 Å early in its history [1985–1987]). We then displaced the transmission curve 3 Å to the blue to account for the temperature difference between the laboratory (24°C) and the telescope (9°C). Shifts due to the converging beam of the telescope (Jacoby *et al.* 1989) were negligible since the telescope is quite slow ($f/13.5$). The current filter response curve, adjusted to the observing temperature, is shown in

TABLE 1
SUMMARY OF STANDARD STAR PHOTOMETRY

UT Date (1)	Number of Observations (2)	Atmospheric Extinction (3)	Zero Point Correction (4)	Standard Error (5)
1989 Nov 10.....	6	0.170	5.843	0.010
1989 Nov 20.....	4	0.155	5.735	0.004
1989 Dec 20.....	3	0.175	5.777	0.026
1989 Dec 21.....	5	0.170	5.776	0.013
1989 Dec 22.....	4	0.180	5.778	0.009
1989 Dec 23.....	5	0.160	5.780	0.010

N

E

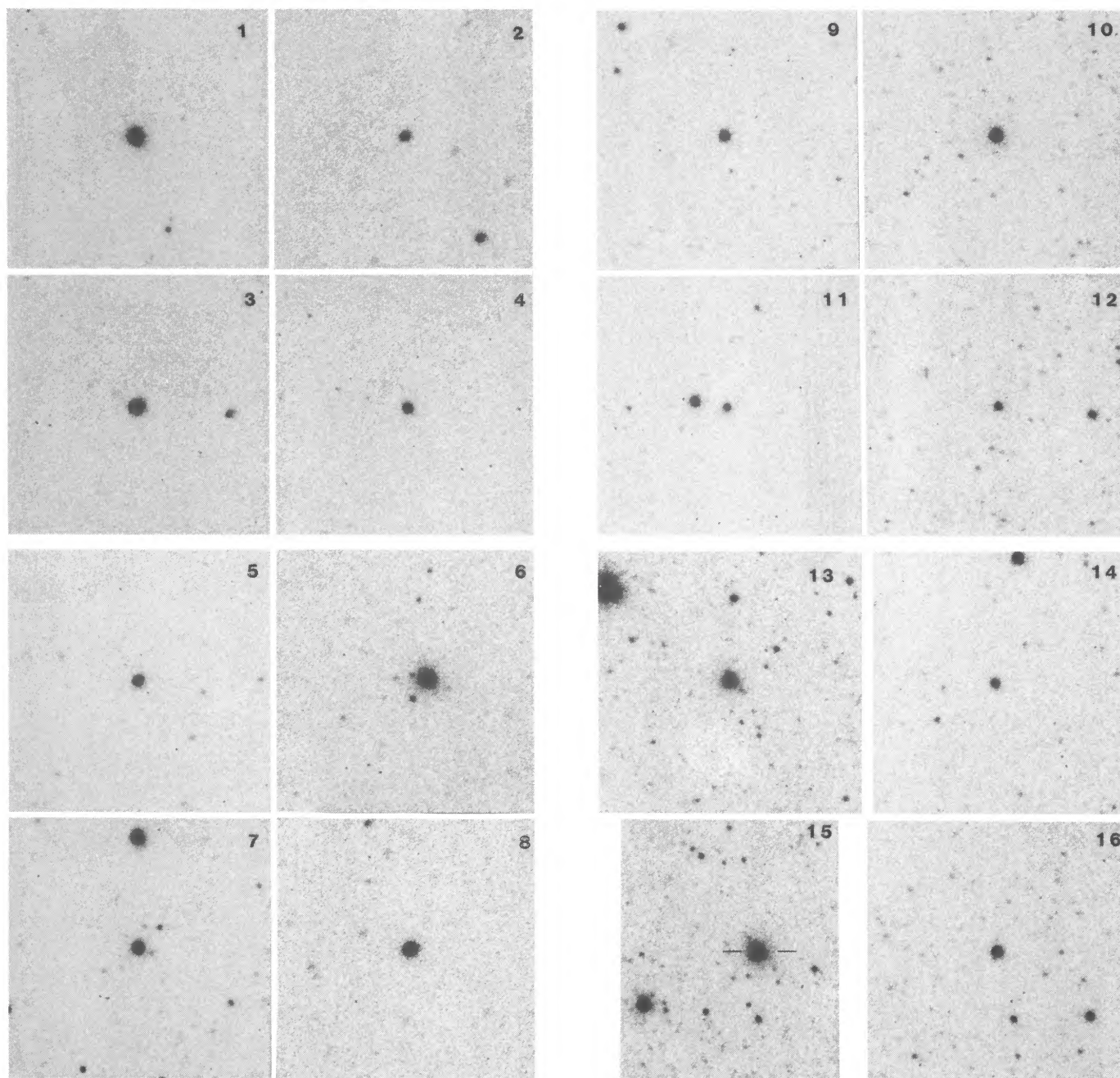


FIG. 1a.—Finding charts for LMC PN SMP 1–16. The PN are the central (usually the brightest) objects in each of these $[\text{O III}] \lambda 5007$ images. All charts are $110'' \times 110''$ except in cases where the PN was found to be near the edge of the CCD frame (e.g., SMP 15).

JACOBY *et al.* (see 365, 472)

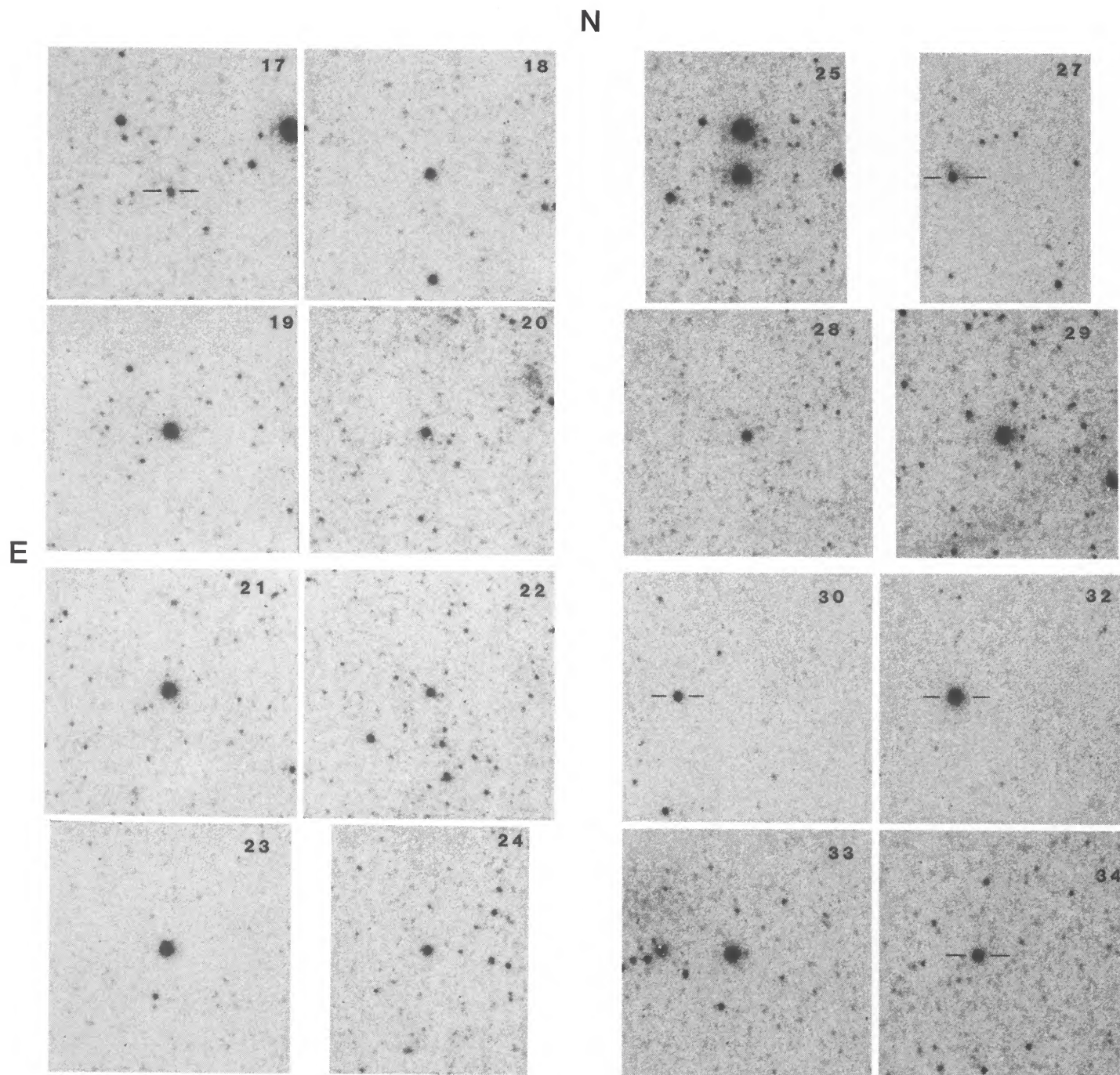


FIG. 1*b*.—Finding charts for LMC PN SMP 17–34. Note that no charts are presented for SMP 26 and 32 since they are extremely faint in $[O\ III]$. When not centrally located in the field, the object is marked (e.g., SMP 17, 27, 30, 32, 34).

JACOBY *et al.* (see 365, 472)

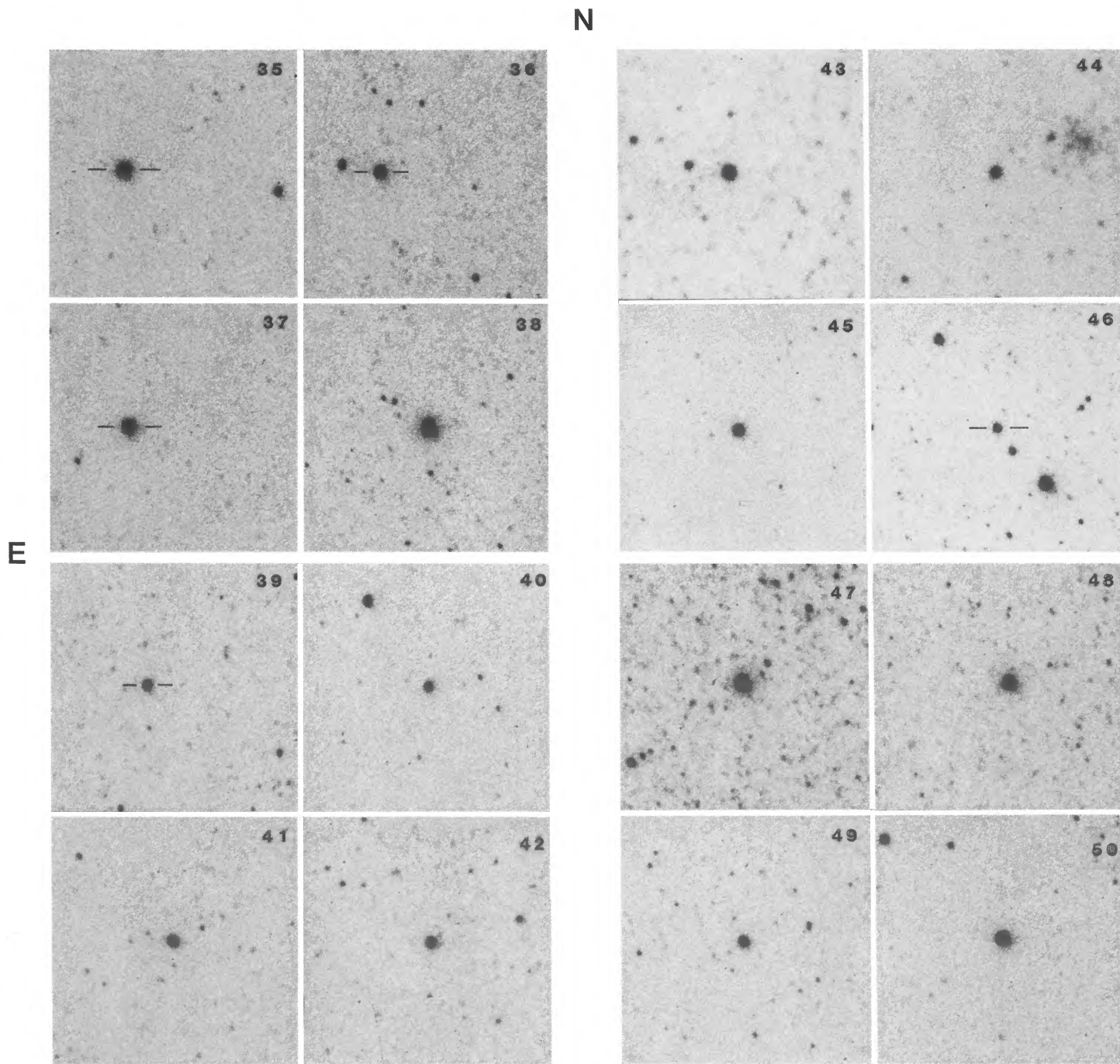


FIG. 1c.—Finding charts for LMC PN SMP 35–50

JACOBY *et al.* (see 365, 472)

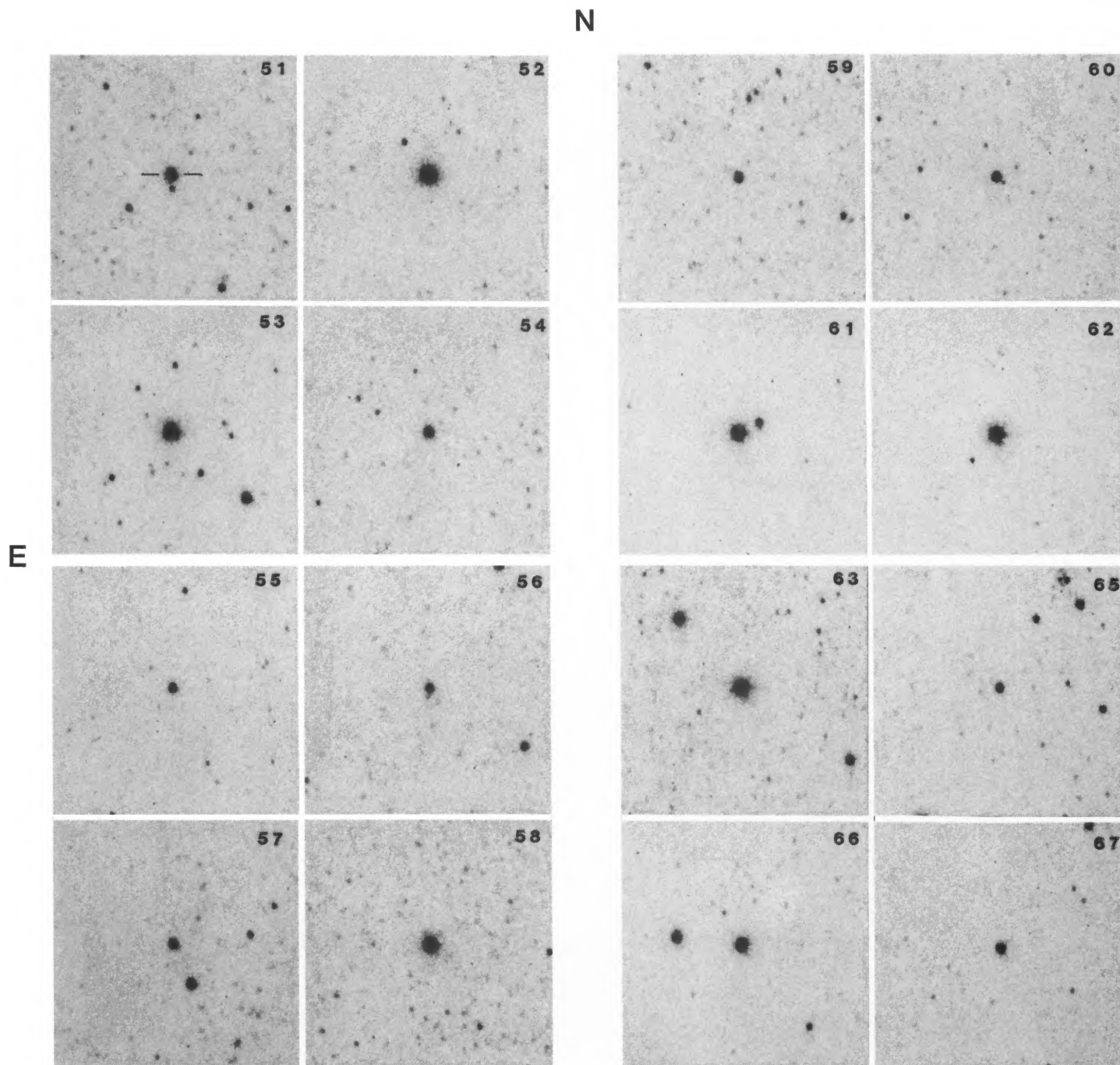


FIG. 1d.—Finding charts for LMC PN SMP 51–67. Note that no chart is presented for SMP 64 since it is extremely faint in $[\text{O III}]$.

JACOBY *et al.* (see 365, 472)

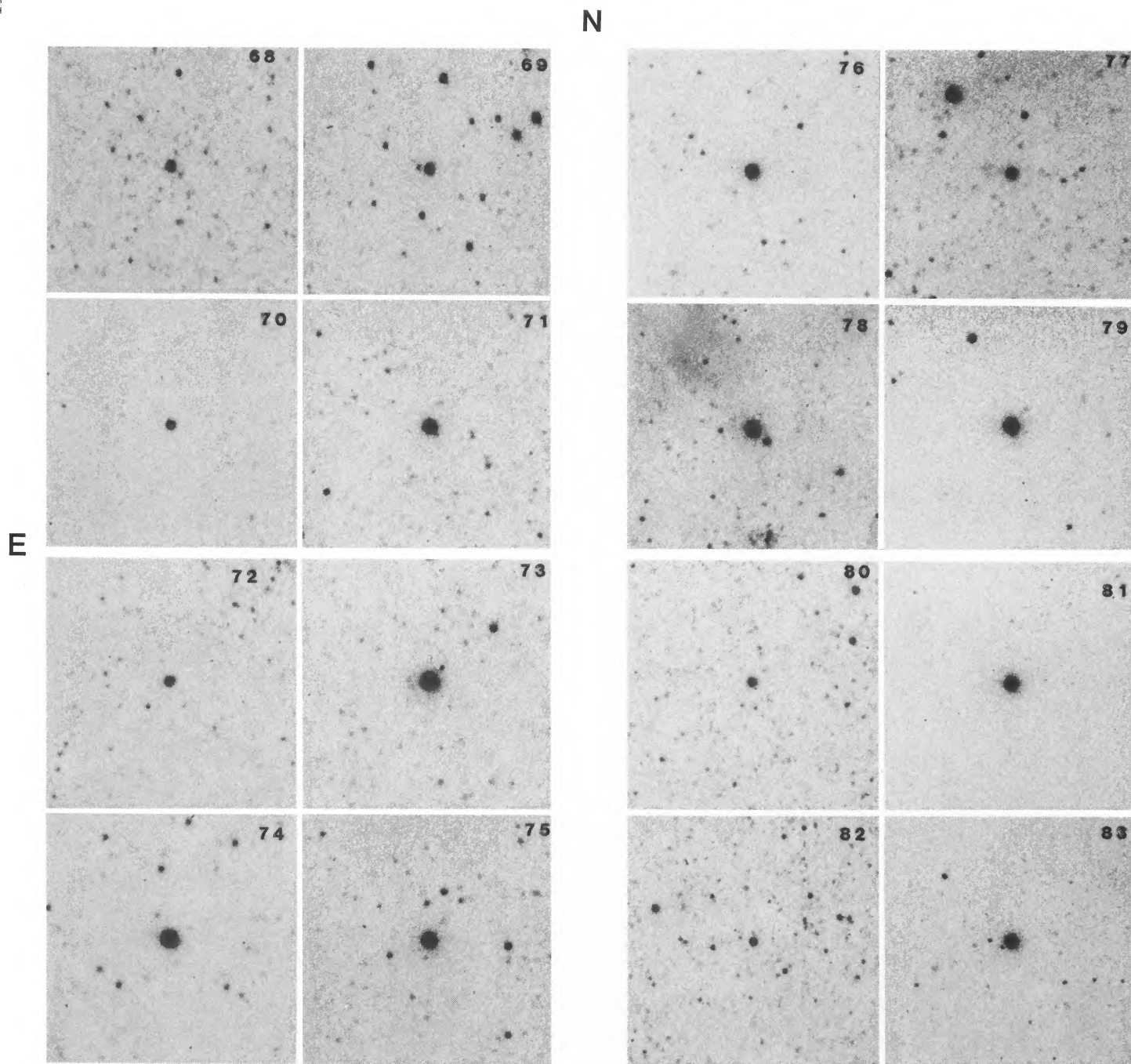


FIG. 1e.—Finding charts for LMC PN SMP 68–83

JACOBY *et al.* (see 365, 472)

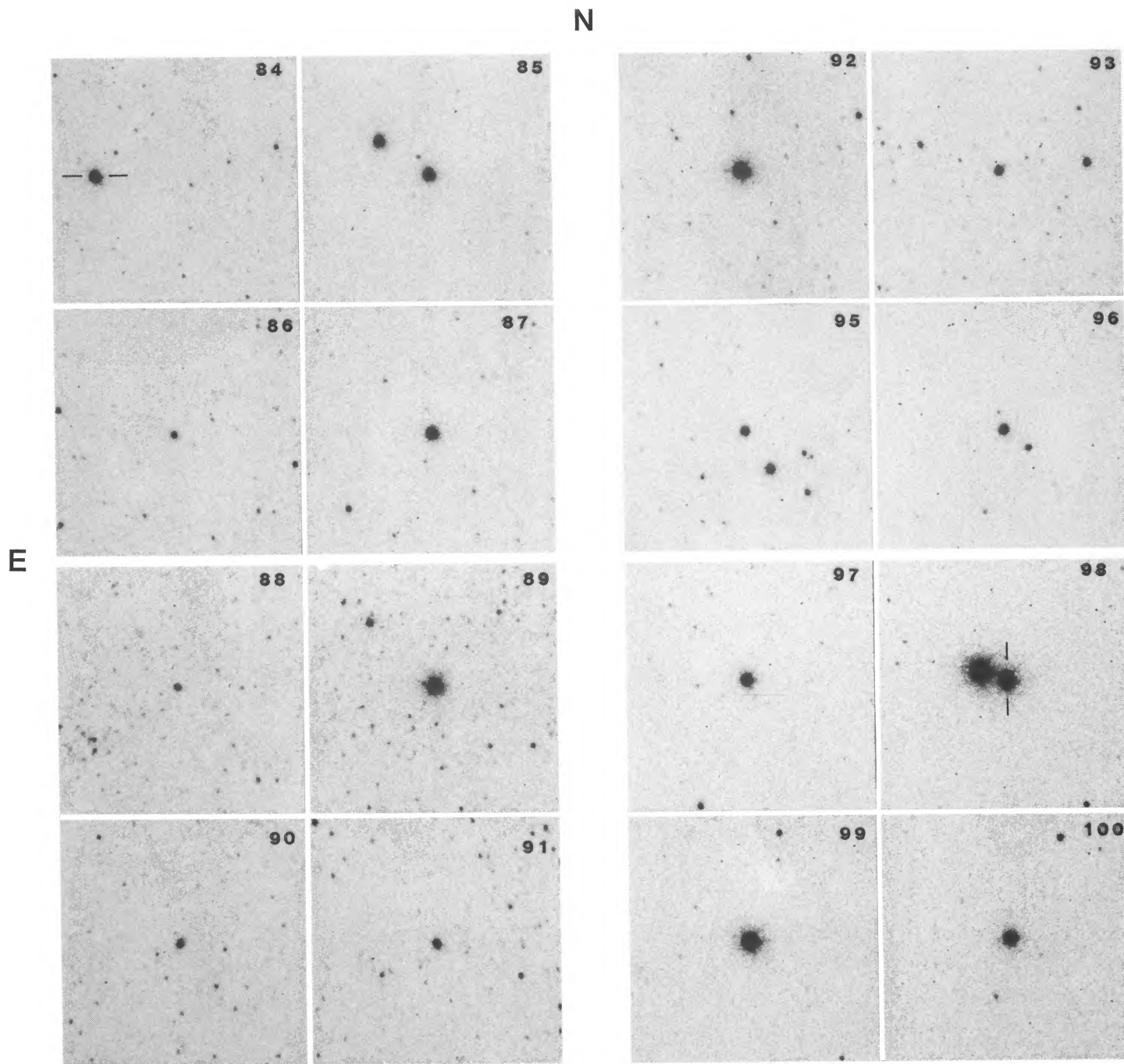


FIG. 1f.—Finding charts for LMC PN SMP 84–100. Note that no chart is presented for SMP 94 since it is extremely faint in $[O\ III]$.

JACOBY *et al.* (see 365, 472)

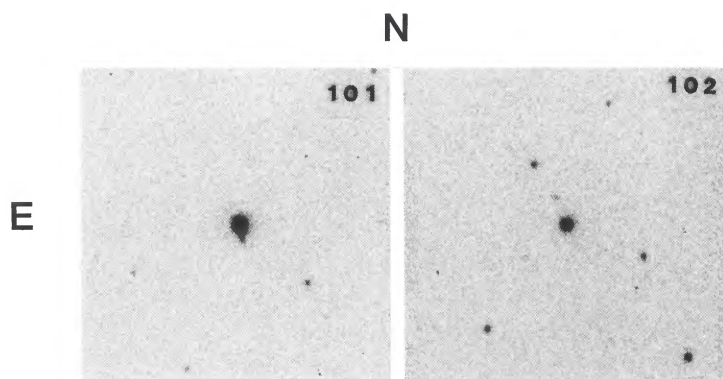


FIG. 1g.—Finding charts for LMC PN SMP 101–102

JACOBY *et al.* (see 365, 472)

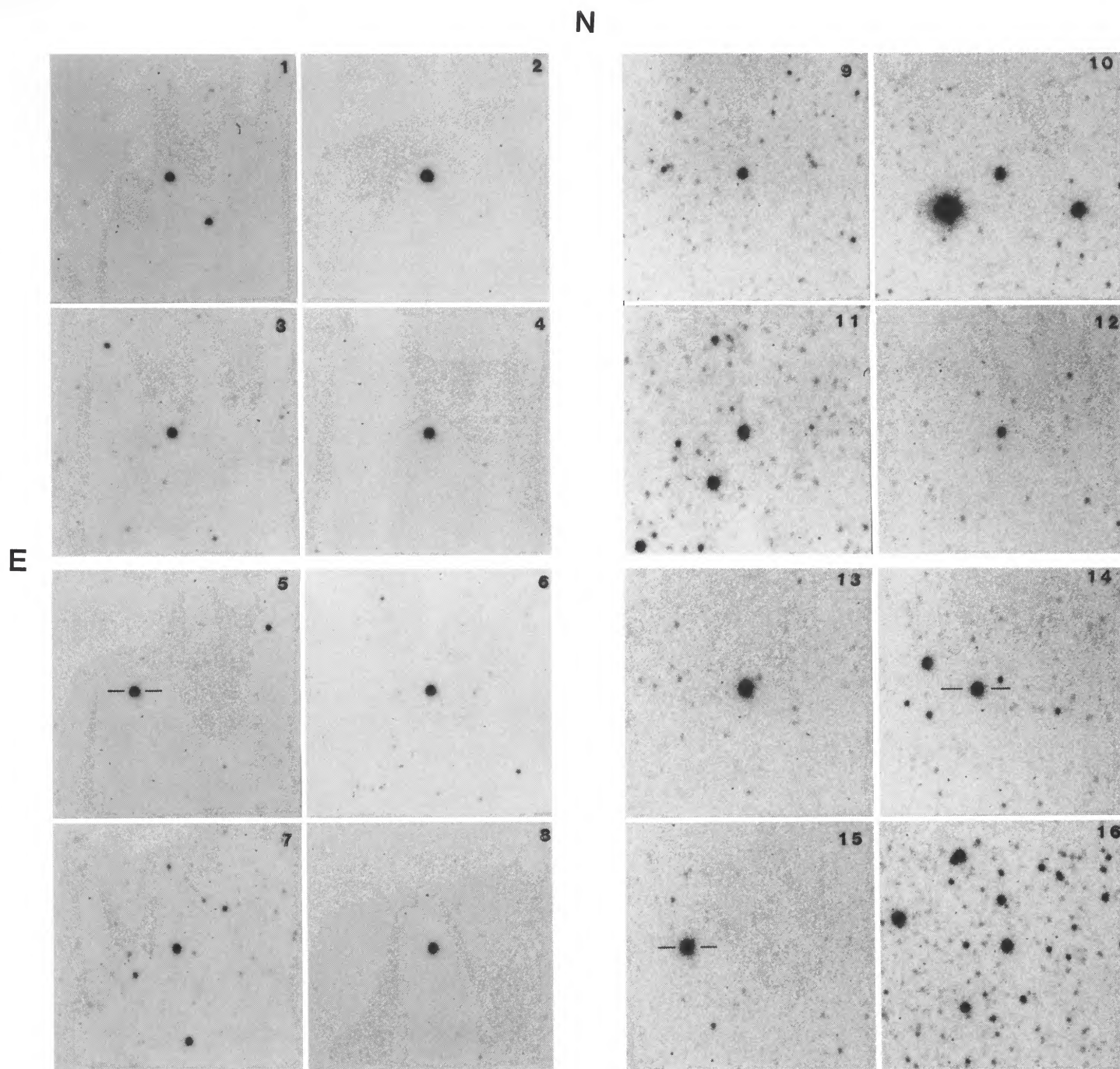


FIG. 2a

FIG. 2.—(a) Finding charts for SMC PN SMP 1–16. (b) Finding charts for SMC PN SMP 17–28, Sanduleak and Pesch (1981) PN 32 and 34, and Lindsay 302.

JACOBY *et al.* (see 365, 472)

N

E

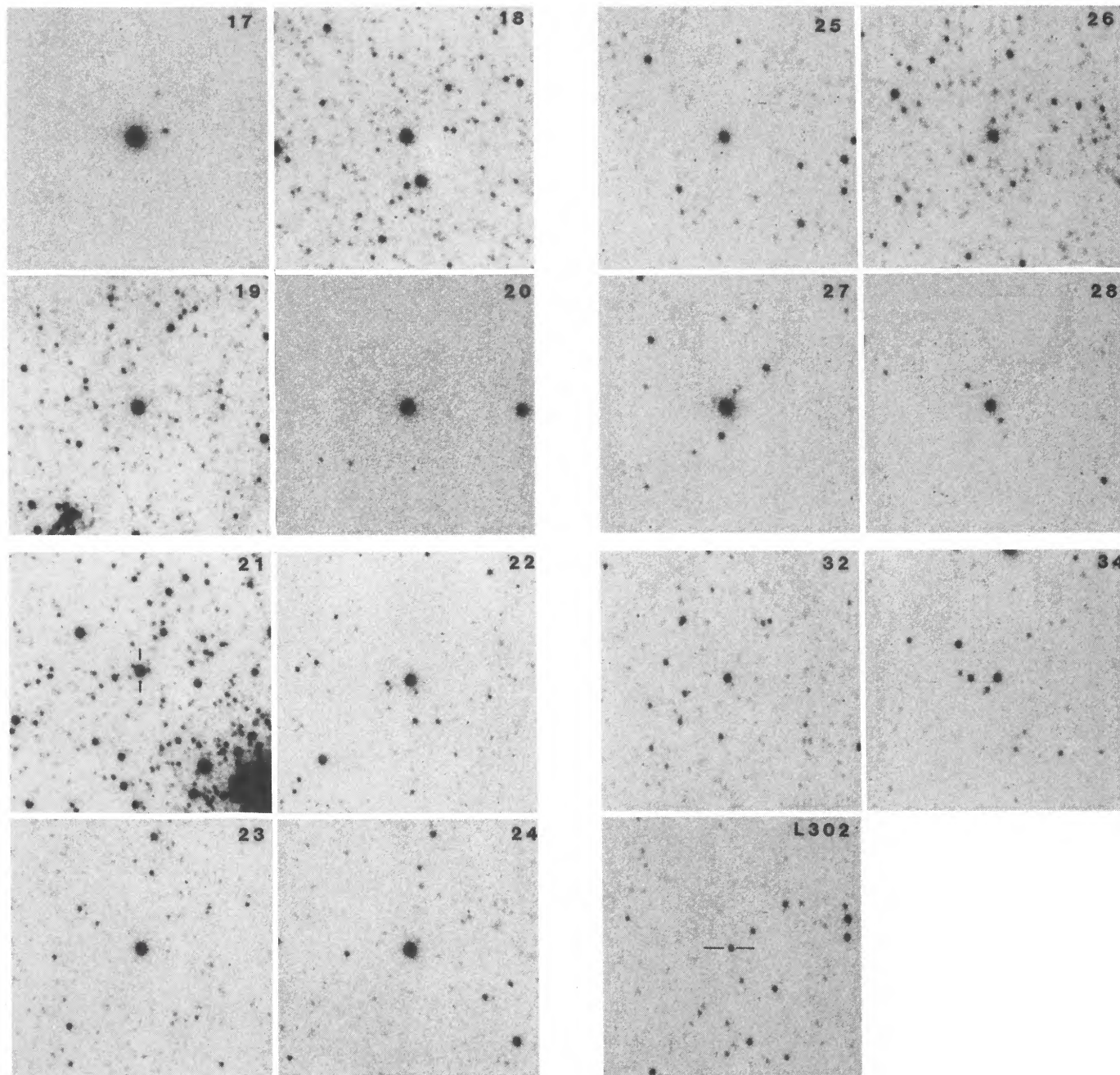


FIG. 2b

JACOBY *et al.* (see 365, 472)

TABLE 2
LMC PLANETARY NEBULA PHOTOMETRY

ID	m_{5007}	$\log F_{5007}$	Velocity (km s ⁻¹)	Diameter (arcsec)	ID	m_{5007}	$\log F_{5007}$	Velocity (km s ⁻¹)	Diameter (arcsec)
SMP 1	15.13	-11.548	224		SMP 52	14.81	-11.421	272	
SMP 2	18.12	-12.744	263		SMP 53	15.07	-11.523	277	
SMP 3	15.90	-11.858	187		SMP 54	17.43	-12.469	280	0.9
SMP 4	17.24	-12.391	298	0.6	SMP 55	17.45	-12.475	210	
SMP 5	17.22	-12.384	286		SMP 56	17.79	-12.611	291	
SMP 6	15.21	-11.580	265		SMP 57	17.59	-12.533	313	
SMP 7	16.39	-12.052	220		SMP 58	15.37	-11.645	279	
SMP 8	16.11	-11.938	293		SMP 59	17.81	-12.622	...	
SMP 9	17.32	-12.424	286		SMP 60	17.29	-12.412	222	1.0
SMP 10	16.34	-12.033	222		SMP 61	15.10	-11.538	193	
SMP 11	18.55	-12.917	265		SMP 62	14.41	-11.261	239	
SMP 12	18.25	-12.797	...		SMP 63	14.89	-11.451	264	
SMP 13	15.77	-11.806	227		SMP 64	>19.38	<-13.248	...	
SMP 14	18.26	-12.802	252	0.9	SMP 65	17.67	-12.565	211	
SMP 15	15.04	-11.513	203		SMP 66	15.78	-11.809	304	
SMP 16	17.04	-12.312	253	0.8	SMP 67	16.93	-12.267	289	
SMP 17	18.80	-13.016	...	1.0	SMP 68	17.05	-12.318	...	0.5
SMP 18	17.43	-12.467	244		SMP 69	17.31	-12.419	305	0.9
SMP 19	15.49	-11.692	235		SMP 70	17.81	-12.619	...	0.8
SMP 20	17.61	-12.542	288		SMP 71	15.71	-11.778	216	
SMP 21	15.58	-11.728	259		SMP 72	17.92	-12.665	...	1.7
SMP 22	17.95	-12.676	...		SMP 73	14.66	-11.359	241	
SMP 23	15.68	-11.769	283		SMP 74	15.19	-11.570	269	
SMP 24	18.14	-12.751	270	1.3	SMP 75	15.07	-11.522	301	
SMP 25	14.84	-11.433	188		SMP 76	15.54	-11.712	278	
SMP 26	>19.43	<-13.268	256		SMP 77	16.57	-12.122	343	
SMP 27	17.50	-12.497	273		SMP 78	14.76	-11.398	256	
SMP 28	17.23	-12.390	249		SMP 79	15.07	-11.526	230	
SMP 29	15.54	-11.714	243		SMP 80	17.24	-12.392	...	
SMP 30	17.86	-12.639	280	0.7	SMP 81	14.91	-11.460	257	
SMP 31	>19.41	<-13.260	263		SMP 82	17.54	-12.510	255	
SMP 32	15.63	-11.750	255		SMP 83	15.63	-11.747	291	1.3
SMP 33	15.63	-11.748	269		SMP 84	15.80	-11.814	250	
SMP 34	16.71	-12.181	267		SMP 85	16.01	-11.899	232	
SMP 35	15.54	-11.713	310	0.7	SMP 86	18.46	-12.879	...	
SMP 36	16.17	-11.965	263		SMP 87	16.12	-11.943	280	0.8
SMP 37	15.77	-11.806	270		SMP 88	17.80	-12.616	226	0.6
SMP 38	14.99	-11.492	240		SMP 89	14.91	-11.460	276	
SMP 39	16.64	-12.152	...		SMP 90	17.97	-12.685	...	1.3
SMP 40	17.00	-12.297	254		SMP 91	17.81	-12.619	310	1.3
SMP 41	16.57	-12.123	259	0.9	SMP 92	14.80	-11.414	271	
SMP 42	16.63	-12.146	288		SMP 93	17.93	-12.669	...	1.8
SMP 43	16.30	-12.016	...		SMP 94	>19.42	<-13.266	272	
SMP 44	17.38	-12.449	...		SMP 95	17.31	-12.421	306	0.6
SMP 45	16.31	-12.022	290	0.6	SMP 96	17.22	-12.385	255	
SMP 46	17.31	-12.419	273		SMP 97	15.94	-11.874	287	0.6
SMP 47	14.94	-11.472	272		SMP 98	14.52	-11.303	264	
SMP 48	15.25	-11.594	256		SMP 99	14.70	-11.377	264	
SMP 49	16.61	-12.142	247		SMP 100	15.70	-11.778	285	0.7
SMP 50	15.40	-11.655	299		SMP 101	15.86	-11.839	281	1.2
SMP 51	16.26	-12.000	271		SMP 102	17.08	-12.326	302	0.8

Figure 3, and the systemic velocities of the LMC and SMC are noted.

Photometry of the PN is listed in Tables 2 (LMC) and 3 (SMC). With the exceptions of L302 and the two Sanduleak and Pesch (1981) objects, the identification in column (1) is that given by SMP, who also list cross references to early catalogs. The [O III] flux has been transformed to the magnitude system defined in our previous papers using the relation

$$m_{5007} = -2.5 \log F_{5007} - 13.74 . \quad (1)$$

The magnitudes as defined by equation (1) are given in column

(2). Column (3) gives the logarithm of the flux for comparison with other authors. LMC PN 26, 31, 64, and 94 are very faint in [O III], and so the values in these columns represent upper limits to their brightness.

When known, the PN radial velocity is listed in column (4) of Tables 2 and 3. In order to calculate the PN line flux, the wavelength of the [O III] emission line is required, together with the filter transmission as a function of wavelength (Jacoby, Quigley, and Africano 1987). For the SMC, the velocities are those determined by Dopita *et al.* (1985). Lindsay 302 has no measured velocity so we have adopted the mean of the

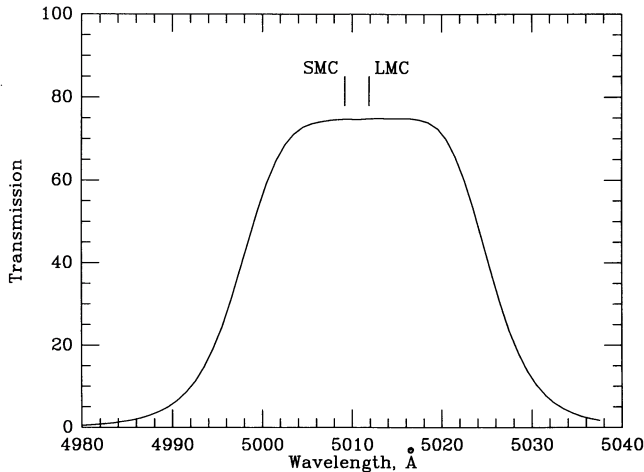


FIG. 3.—The transmission curve for the [O III] narrow-band filter at the usual nightly temperature of 9°C. The systemic velocities of the LMC and SMC are noted.

others, 141 km s⁻¹. For the LMC, most of the PN have velocities measured by Meatheringham *et al.* (1988). Five additional PN have unpublished velocities measured by one of us (A. R. W.) using the IPCS and Unit Spectrograph on the SAAO 1.9 m telescope, while 15 PN have no measured velocity. We assume a velocity of 260 km s⁻¹ for these latter PN. The response function of the filter, measured immediately after the December observing run, showed a variation of only 1.5% over the

TABLE 3

SMALL MAGELLANIC CLOUD PLANETARY NEBULA PHOTOMETRY

ID (1)	m_{5007} (2)	$\log F_{5007}$ (3)	Velocity (km s ⁻¹) (4)	Diameter (arcsec) (5)
SMP 1	17.29	-12.412	147	
SMP 2	15.58	-11.728	157	1.1
SMP 3	16.74	-12.192	123	
SMP 4	16.43	-12.070	168	
SMP 5	15.72	-11.783	110	
SMP 6	15.91	-11.861	156	
SMP 7	17.64	-12.554	143	0.6
SMP 8	16.23	-11.990	125	
SMP 9	17.32	-12.426	175	0.6
SMP 10	16.60	-12.134	137	
SMP 11	17.30	-12.416	137	1.0
SMP 12	18.04	-12.711	122	0.7
SMP 13	15.31	-11.620	153	
SMP 14	16.35	-12.035	204	0.5
SMP 15	15.40	-11.655	114	
SMP 16	17.51	-12.499	124	
SMP 17	15.15	-11.557	105	
SMP 18	16.57	-12.124	122	
SMP 19	16.41	-12.062	109	
SMP 20	15.76	-11.802	99	
SMP 21	17.25	-12.395	160	
SMP 22	17.33	-12.426	153	0.6
SMP 23	16.81	-12.222	122	
SMP 24	16.21	-11.980	140	
SMP 25	18.01	-12.701	146	
SMP 26	18.08	-12.726	196	
SMP 27	15.49	-11.694	105	
SMP 28	18.03	-12.708	182	
SP 32	18.52	-12.902	169	
SP 34	18.53	-12.909	126	
L302	19.33	-13.227	...	

entire velocity range of 99 km s⁻¹ to 343 km s⁻¹, so flux errors arising from uncertainties in the PN velocities are negligible.

Column (5) gives an estimate of the FWHM diameter for those objects which appear slightly nonstellar. Following Wood *et al.* (1987), we calculated the diameters by subtracting the FWHM of stars in the frame from the PN FWHM in quadrature. Our diameters correlate very well with those of Wood *et al.* (1987), although our values are typically ~ 0.3 smaller.

Due to a lack of observing time, it was not possible to make repeat observations of all the PN in order to determine the external error as a function of magnitude. (LMC PN 19 and 32 were observed twice, and the differences between measurements were 0.05 and 0.01 mag, respectively.) For the brighter PN it is certainly true that the actual error is much larger than the formal error of the photometry. Probably, the best estimate for the limiting accuracy of our photometry comes from the scatter in the measurements for the bright standard stars (typically 0.015 mag). Therefore we convolved 0.015 mag in quadrature with error estimates determined from the photometric counting statistics to arrive at the external error as a function of PN magnitude. These are listed in Table 4.

A few PN have very weak [O III] emission and could not be measured. Most of these objects have very low excitation; however, unusual PN do exist such as LMC 94, which has high excitation but no [O III] emission. Also, faint PN may have bright central stars whose continua contribute to the apparent [O III] fluxes. This effect, however, is never more than a few percent even in the most extreme cases, thanks to the continuum suppression provided by the narrow-band filter. Since we are interested only in the bright end of the luminosity function when deriving distances, these PN do not enter in the subsequent analysis.

d) Comparison with Other Photometry

As a check, we have compared our fluxes with those published by Webster (1969, 1976, 1983), Osmer (1976), Wood *et al.* (1987), Barlow (1987), and Meatheringham, Dopita, and Morgan (1988). For most objects, only H β fluxes are available, but these can be transformed into [O III] fluxes using spectra in the literature (Monk, Barlow, and Clegg 1988). Note that it is necessary to adjust the zero point of some of these data sets by -0.03 in log flux (Shaw and Kaler 1989; Webster 1983) to account for revisions to the absolute flux calibration of Vega (Hayes and Latham 1975).

Table 5 summarizes the comparisons between the data published by these authors and the data presented here. In short, there appear to be zero-point differences of ~ 0.03 in the

TABLE 4
PHOTOMETRIC ERROR VERSUS
MAGNITUDE

m_{5007}	Internal Error	Total Error
15.0	0.004	0.015
15.5	0.005	0.016
16.0	0.006	0.016
16.5	0.008	0.017
17.0	0.009	0.017
17.5	0.013	0.020
18.0	0.025	0.030
18.5	0.035	0.040
19.0	0.050	0.050

TABLE 5
COMPARISON OF [O III] λ 5007 LOG FLUXES

Reference	Number of Objects	Zero Point Difference	rms Dispersion	Notes
Webster 1969	26	+0.00	0.02	1
Webster 1976	13	+0.03	0.03	1
Webster 1983	6	+0.04	0.01	
Osmer 1976	6	-0.03	0.03	1
Meatheringham, Dopita, and Morgan 1988	58	-0.03	0.05	1, 2
Wood <i>et al.</i> 1987	11	+0.03	0.06	1, 2

NOTES.—(1) Fluxes adjusted by -0.03 in the log; (2) $H\beta$ fluxes converted to [O III] λ 5007 using spectra from Monk, Barlow, and Clegg 1988.

log of the flux. Systematic errors of this magnitude are generally not seen in photometry of stellar sources, and we hypothesize that the larger errors stem from the difficulty in calibrating narrow-band filter response curves.

The internal consistency (rms dispersion) is slightly better, in general, but there are several objects for which large discrepancies persist. The most notable examples are SMC objects SMP 24 for which Webster (1969, 1976, 1983) presents log [O III] fluxes of -12.02 , -12.12 , and -12.17 , while we obtain -12.04 . The situation for L302 is even more dramatic; Webster (1983) gives -12.50 while we obtain -13.29 , a difference of nearly 2 magnitudes and far larger than our expected error of ~ 0.1 mag for this object.

Table 5 also shows that the [O III] fluxes derived by combining spectral line ratios with $H\beta$ fluxes are inferior, having an internal consistency of ~ 0.05 (rms dispersion) in the log. By comparison, direct photometry in [O III] exhibits a dispersion of ~ 0.02 in the log. This additional error is consistent with the usual uncertainties ($\sim 10\%$) in spectroscopy. After applying the [O III]/ $H\beta$ line ratios to the $H\beta$ photometry by Meatheringham, Dopita, and Morgan (1988), we find that LMC objects SMP 3 and SMP 8 are highly discrepant, apparently due to typographical errors in the $H\beta$ fluxes. These $H\beta$ fluxes should be -12.48 and -12.74 respectively (S. J. Meatheringham 1990, private communication). In addition, SMP 36 is discordant by 0.47 in the log, but we have no explanation in this case. Webster (1983) points out that differences in the photometry have led to suspicions of PN variability, but follow-up photometry has not identified any truly variable PN among this sample.

e) Extinction

In our previous papers, we have applied the PNLF technique only to old populations where the effects of dust internal to the PN host galaxy are considered to be negligible. When applying the method to the MC where the presence of a young population is obvious, the extinction present in the LMC and SMC must be considered. In fact, the proper approach is to correct each PN individually for the extinction along the line of sight. Unfortunately, only a small fraction of the required data needed to perform this correction is available in the literature.

The determination of extinction to PN is usually accomplished by measuring the Balmer decrement ($H\alpha/H\beta$) and comparing this ratio to the expected value, typically 2.85 (Brocklehurst 1971). Unfortunately, from most observatories, the MC are observable only at large zenith angles, and the effects of atmospheric dispersion on slit spectroscopy are severe (cf. Monk, Barlow, and Clegg 1988). The use of a wide slit eliminates this problem, but at the cost of longer integration times to overcome the additional sky noise.

To estimate mean values of the logarithmic extinction, c , we began by averaging the measurements given by Osmer (1976), Dufour and Killen (1977), Aller *et al.* (1987), and Boroson and Liebert (1989). These comprise a sample of 15 objects in each of the LMC and SMC. In the few cases where more than one measurement is available (LMC 21, 78, and 97; SMC 2, 20, 22), we simply used the average. We then computed grand averages of 0.19 ± 0.17 and 0.08 ± 0.13 for the LMC and SMC, respectively, where the quoted uncertainties are 1σ standard deviations.

We can compare these average values with estimates in the literature. For example, Kaler and Jacoby (1990) used a similar approach to derive average extinction values of 0.21 and 0.12 to the LMC and SMC, respectively. Barlow (1987) used an indirect estimator based on H I observations in the LMC (Rohlfis *et al.* 1984) and SMC (Hindman 1967) combined with the reddening maps of Burstein and Heiles (1982) to derive average extinction values of 0.17 and 0.08.

Adopting another approach, we note that $c \sim 1.44E(B-V)$ (Kaler and Lutz 1985); consequently the above values for c correspond to $E(B-V)$ of 0.13 and 0.06 mag. This relation allows us to improve our estimate of the extinction by combining broad-band reddening estimates in the literature with monochromatic extinction estimates. For example, the above $E(B-V)$ values are somewhat higher than the estimates of 0.074 and 0.054 mag obtained by Caldwell and Coulson (1985). Conti, Garmany, and Massey (1986) find $E(B-V) = 0.11$ mag for B stars in the LMC, and Da Costa and Mould (1986) find $E(B-V) = 0.04$ mag for the SMC cluster NGC 411. (Note that reddening estimates based on young star measurements may be biased to large values if there is an association with gas and dust.) Thus the values adopted for the PN appear to be in good agreement for the SMC, but the LMC values are 0.02–0.04 mag higher than predicted by broad-band estimators. Therefore, we adopt an SMC differential extinction of $E(B-V) = 0.06$, and average the broad-band and PN estimates to yield an LMC reddening of $E(B-V) = 0.10$ mag. We estimate the uncertainty in these numbers to be approximately 0.03 mag for the LMC and 0.01 for the SMC. Using the wavelength-extinction dependence given by Seaton (1979), these reddening values correspond to extinctions at λ 5007 of 0.36 ± 0.11 for the LMC and 0.21 ± 0.04 for the SMC.

III. THE DISTANCE TO THE LMC

The distances to the LMC and SMC are derived using the method of maximum likelihood (Ciardullo *et al.* 1989) to fit the observed PNLF for each galaxy to a model PNLF based on observations of PN in the bulge of M31. We have already defined the quantities which are generally necessary: the extinction corrections, the photometric error function, and the

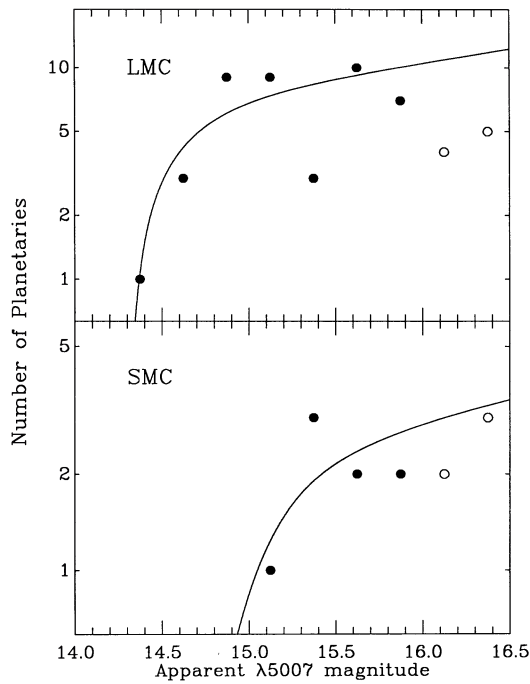


FIG. 4.—The planetary nebula luminosity functions for the LMC (*top*) and SMC (*bottom*) binned into intervals of 0.25 mag. Magnitudes are defined in eq. (1). These samples are probably complete to ~ 2 mag below the brightest PN. Also shown are the models for the PNLF (Ciardullo *et al.* 1989), which have been adjusted for extinction, convolved with the photometric and depth uncertainties (see text), and shifted to the most probable distance moduli of 18.44 and 19.09. Filled circles represent objects brighter than our adopted completeness limit; open circles are below this level and were excluded from the fit.

statistical sample. For the case of the Clouds, however, we must also consider the effect of the depth along the line of sight. Since we do not know, *a priori*, whether a PN is toward the front or back of the galaxy, depth can be treated as a random photometric error. For the LMC, we adopt a 1σ depth uncertainty of 0.04 mag based on the inclination of the galaxy; for the SMC, we adopt 0.18 mag (Feast 1989) based on the spread in Cepheid distances.

The PNLFs for the two galaxies are shown in Figure 4. The model PNLF from Ciardullo *et al.* (1989), corrected for extinction, convolved with the photometric errors (including the depth uncertainty), and shifted to the best-fit distances and sample sizes, is overlaid in the figure. It is apparent that the PNLF in the SMC is extremely sparse; the PNLF for the LMC is better populated, but the sample size is still much smaller than we usually realize. Consequently, while we can derive a distance to the LMC which has a modest internal uncertainty, the derived distance to the SMC carries much less significance. The maximum likelihood solutions for the two galaxies are shown in Figure 5.

We see from the figures that the derived distance modulus for the LMC is 18.44 ± 0.08 , and that for the SMC is $19.09^{+0.25}_{-0.32}$, where the quoted errors represent the 1σ internal errors of the fit. To calculate the true uncertainty, we must add to these errors any potential systematic errors introduced by the uncertainties in the distance to the calibrator galaxy, M31 (0.1 mag), our ability to define the zero point and shape of the model PNLF (0.05 mag), our estimates for the extinction correction (0.11 and 0.04 mag for the LMC and SMC, respectively), and our definition of the photometric zero point

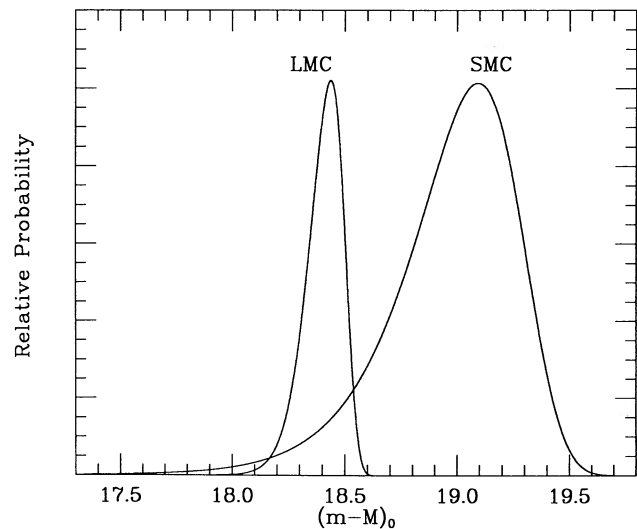


FIG. 5.—The results from the maximum likelihood solutions for the LMC and SMC PNLFs. The abscissa is the true distance modulus; the ordinate is the probability that the observed PNLF is drawn from the empirical model (Ciardullo *et al.* 1989) at the given distance. Corrections for extinction, photometric error, and depth uncertainty have been applied.

(0.03 mag). These correspond to net systematic uncertainties of 0.16 and 0.12 mag, which when included with the formal errors of the fit yield distance moduli of 18.44 ± 0.18 and $19.4^{+0.25}_{-0.32}$ for the LMC and SMC, respectively.

We compare the LMC value to other recent determinations in Table 6. Note that the entries in this table have not been adjusted for the different extinction estimates adopted by the authors, and these vary from $E(B-V) = 0.06$ to $E(B-V) = 0.12$. Nevertheless, we feel that the entries in Table 6 are representative of the state of distance determinations to the LMC, the galaxy whose distance is probably the most accurately known. To summarize the implications of the table, the PNLF distance for the LMC is in excellent agreement with Cepheid distances derived from either optical or infrared observations. This is extremely encouraging in that the PNLF was calibrated solely on the Cepheid distance to M31. Thus the external consistency of distances derived using the PNLF method is as good as that of Cepheids.

This is a remarkable result for the following three reasons. First, the Hubble type of the LMC (historically Irr I, but now classified as SBm) is distinctly different than that of M31 (Sb), indicating that the PNLF method is insensitive to host galaxy

TABLE 6
SUMMARY OF RECENT DISTANCE ESTIMATES
TO THE LARGE MAGELLANIC CLOUD

Method	Distance Modulus
Cepheids (Feast and Walker 1987)	18.47 ± 0.15
Cepheids (Welch <i>et al.</i> 1987)	18.57 ± 0.05
RR Lyraes (Reid and Strugnell 1986)	18.37 ± 0.15
RR Lyraes (Walker and Mack 1987)	18.44 ± 0.05
MS fitting (Schommer, Olszewski, and Aaronson 1984)	18.2 ± 0.2
MS fitting (Chiosi and Pigatto 1986)	18.5 ± 0.1
O stars (Conti, Garmany, and Massey 1986)	18.3 ± 0.3
B stars (Shobbrock and Visvanathan 1987)	18.3 ± 0.2
Miras (Feast 1988)	18.28 ± 0.1
Novae (Capaccioli <i>et al.</i> 1990)	18.70 ± 0.2
PNLF (This paper)	18.44 ± 0.18

morphology. Second, as evidenced by the difference between the $B-V$ colors of the LMC (0.55; Bothun and Thompson 1988) and M31's bulge (0.9; Sandage, Becklin, and Neugebauer 1969), the population mix of the LMC is extremely young. This indicates that the PNLF is insensitive to the details of the star formation history of the host galaxy. Third, the metallicity of the older stars in the LMC (presumably the progenitors of the PN) is approximately a factor of 2 below solar (Spite 1989). The metallicity of the bulge of M31, by contrast, is approximately a factor of 2 above solar (based on the Mg_2 index from Burstein *et al.* 1988 and the calibration by Terlevich *et al.* 1981). Thus, the PNLF method is also insensitive to the metallicity of the host galaxy.

The PNLF distance to the SMC, on the other hand, does not carry much weight; only 10 PN fall in the critical first mag of the PNLF, as compared to 24 for the LMC. From past usage of the method (cf. Ciardullo *et al.* 1989), we have found that 20–30 PN are needed in this range to yield a reliable result. Nevertheless, we can compare our differential between the LMC and SMC with other determinations. Most investigators place the SMC at an average distance modulus of ~ 0.5 mag farther than the LMC (Feast 1988). Feast (1989), however, notes that the SMC may be elongated along the line of sight, having a total extent of ~ 0.7 mag in distance modulus. Our results, if taken at face value, indicate that the SMC is 0.65 mag farther, or 1σ from the accepted difference. Considering the

small number of objects in our SMC sample, and the considerable uncertainty introduced by the effects of depth, we do not consider our difference of 0.65 mag to be significantly greater.

Finally, we note that Pottasch (1990) has recently derived the distance to the Galactic center (8.1 kpc) using the PNLF method with M31 as the calibrator. This result provides yet another verification of the PNLF technique in a late-type galaxy (the Milky Way). Pottasch also found that when he calibrated the PNLF with LMC PN (at an assumed distance modulus of 18.36), he also derived this distance to the Galactic center. Thus, he indirectly confirmed the distance to the LMC using the PNLF method.

IV. CONCLUSIONS

We have presented accurate $[O\ III]\ \lambda 5007$ fluxes for 133 bright PN in the MC and derived distances using the PNLF method. Our distance to the LMC agrees extremely well with other recent determinations and is essentially identical to the Cepheid distance. We cannot derive an accurate distance to the SMC, however, due to the small number of bright PN in that galaxy.

With this new PNLF distance to the LMC, we have now added a second calibrator galaxy for the method. Of greater importance, the consistency of the PNLF method as compared to other reliable indicators shows that the method is insensitive to host galaxy Hubble type, color, or chemical composition.

REFERENCES

- Aller, L. H., Keyes, C. D., Maran, S. P., Gull, T. R., Michalitsianos, A. G., and Stecher, T. P. 1987, *Ap. J.*, **320**, 159.
 Barlow, M. J. 1987, *M.N.R.A.S.*, **227**, 161.
 Boroson, T. A., and Liebert, J. 1989, *Ap. J.*, **339**, 844.
 Bothun, G. D., and Thompson, I. B. 1988, *A.J.*, **96**, 877.
 Brocklehurst, M. 1971, *M.N.R.A.S.*, **153**, 471.
 Burstein, D., Bertola, F., Buson, L. M., Faber, S. M., and Lauer, T. R. 1988, *Ap. J.*, **328**, 440.
 Burstein, D., and Heiles, C. 1982, *A.J.*, **87**, 1165.
 Caldwell, J. A. R., and Coulson, I. M. 1986, *M.N.R.A.S.*, **218**, 223.
 Capaccioli, M., Della Valle, M., D'Onofrio, M., and Rosino, L. 1990, *Ap. J.*, **360**, 63.
 Chiosi, C., and Pigatto, L. 1986, *Ap. J.*, **308**, 1.
 Ciardullo, R., Jacoby, G. H., and Ford, H. C. 1989, *Ap. J.*, **344**, 715.
 Ciardullo, R., Jacoby, G. H., Ford, H. C., and Neill, J. D. 1989, *Ap. J.*, **339**, 53.
 Conti, P. S., Garmany, C. D., and Massey, P. 1986, *A.J.*, **92**, 48.
 Da Costa, G. S., and Mould, J. R. 1986, *Ap. J.*, **305**, 214.
 Ditsler, W. 1990, in *CCDs in Astronomy* (A.S.P. Conference Series No. 8), ed. G. H. Jacoby (San Francisco: A.S.P.), p. 126.
 Dopita, M. A., Ford, H. C., Lawrence, C. J., and Webster, B. L. 1985, *Ap. J.*, **296**, 390.
 Dufour, R. J., and Killen, R. M. 1977, *Ap. J.*, **211**, 68.
 Feast, M. W. 1988, in *The Extragalactic Distance Scale* (A.S.P. Conference Series No. 4), ed. S. van den Bergh and C. J. Pritchet (Provo: Brigham Young University Press), p. 9.
 ———. 1989, in *Recent Developments of Magellanic Cloud Research*, ed. K. S. de Boer, F. Spite, and G. Stasińska (Meudon: l'Observatoire de Paris), p. 75.
 Feast, M. W., and Walker, A. R. 1987, *Ann. Rev. Astr. Ap.*, **25**, 345.
 Hayes, D. S., and Latham, D. W. 1975, *Ap. J.*, **197**, 593.
 Henize, K. G. 1956, *Ap. J. Suppl.*, **2**, 315.
 Hindman, J. V. 1967, *Australian J. Phys.*, **20**, 147.
 Jacoby, G. H. 1980, *Ap. J. Suppl.*, **42**, 1.
 Jacoby, G. H. 1989, *Ap. J.*, **339**, 39.
 Jacoby, G. H., Ciardullo, R., and Ford, H. C. 1990, *Ap. J.*, **356**, 332.
 Jacoby, G. H., Ciardullo, R., Ford, H. C., and Booth, J. 1989, *Ap. J.*, **344**, 704.
 Jacoby, G. H., and Ford, H. C. 1986, *Ap. J.*, **304**, 490.
 Jacoby, G. H., Quigley, R. J., and Africano, J. L. 1987, *Pub. A.S.P.*, **99**, 672.
 Kaler, J. B., and Jacoby, G. H. 1990, *Ap. J.*, **362**, 176.
 Kaler, J. B., and Lutz, J. H. 1985, *Pub. A.S.P.*, **97**, 700.
 Lindsay, E. M. 1961, *A.J.*, **66**, 169.
 ———. 1963, *Irish Astr. J.*, **6**, 127.
 Meatheringham, S. J., Dopita, M. A., Ford, H. C., and Webster, B. L. 1988, *Ap. J.*, **327**, 651.
 Meatheringham, S. J., Dopita, M. A., and Morgan, D. H. 1988, *Ap. J.*, **329**, 166.
 Monk, D. J., Barlow, M. J., and Clegg, R. E. S. 1988, *M.N.R.A.S.*, **234**, 583.
 Morgan, D. H., and Good, A. R. 1985, *M.N.R.A.S.*, **213**, 419.
 Mould, J. 1988, in *The Extragalactic Distance Scale* (A.S.P. Conference Series No. 4), ed. S. van den Bergh and C. J. Pritchet (Provo: Brigham Young University Press), p. 32.
 Oke, J. B., Harris, F. H., Oke, D. C., and Wang, Delong 1988, *Pub. A.S.P.*, **100**, 116.
 Osmer, P. S. 1976, *Ap. J.*, **203**, 352.
 Pottasch, S. R. 1990, *Astr. Ap.*, **236**, 231.
 Reid, I. N., and Strugnell, P. R. 1986, *M.N.R.A.S.*, **221**, 887.
 Rohlf, K., Kreitschmann, J., Seigman, B. C., and Feitzinger, J. V. 1984, *Astr. Ap.*, **137**, 343.
 Sandage, A. R., Becklin, E. E., and Neugebauer, G. 1969, *Ap. J.*, **157**, 55.
 Sanduleak, N., MacConnell, D. J., and Philip, A. G. D. 1978, *Pub. A.S.P.*, **90**, 621 (SMP).
 Sanduleak, N., and Pesch, P. 1981, *Pub. A.S.P.*, **93**, 431.
 Schommer, R. A., Olszewski, E. W., and Aaronson, M. 1984, *Ap. J. (Letters)*, **285**, L53.
 Seaton, M. J. 1979, *M.N.R.A.S.*, **187**, 73P.
 Shaw, R. A., and Kaler, J. B. 1989, *Ap. J. Suppl.*, **69**, 495.
 Shobbrock, R. R., and Visvanathan, N. 1987, *M.N.R.A.S.*, **225**, 947.
 Spite, F. 1989, in *Recent Developments of Magellanic Cloud Research*, ed. K. S. de Boer, F. Spite, and G. Stasińska (Meudon: l'Observatoire de Paris), p. 39.
 Stone, R. P. S., and Baldwin, J. E. 1983, *M.N.R.A.S.*, **204**, 347.
 Terlevich, R., Davies, R. L., Faber, S. M., and Burstein, D. 1981, *M.N.R.A.S.*, **196**, 381.
 Walker, A. R. 1984, *M.N.R.A.S.*, **209**, 83.
 Walker, A. R., and Mack, P. 1988, *A.J.*, **96**, 1362.
 Webster, B. L. 1969, *M.N.R.A.S.*, **143**, 79.
 ———. 1976, *M.N.R.A.S.*, **174**, 513.
 ———. 1983, *Pub. A.S.P.*, **95**, 610.
 Welch, D. L., McAlary, C. W., McLaren, R. A., and Madore, B. F. 1986, *Ap. J.*, **305**, 583.
 Welch, D. L., McLaren, R. A., Madore, B. F., and McAlary, C. W. 1987, *Ap. J.*, **321**, 162.
 Westerlund, B. E. 1968, in *IAU Symposium 34, Planetary Nebulae*, ed. D. E. Osterbrock and C. R. O'Dell (Dordrecht: Reidel), p. 23.
 Wood, P. R., Meatheringham, S. J., Dopita, M. A., and Morgan, D. H. 1987, *Ap. J.*, **320**, 178.

ROBIN CIARDULLO and GEORGE H. JACOBY: Kitt Peak National Observatory, P.O. Box 26732, Tucson, AZ 85726

ALISTAIR R. WALKER: Cerro Tololo Inter-American Observatory, Casilla 603, La Serena, Chile 1353